Available online www.unicrossjournals.com

UNICROSS JOURNAL OF SCIENCE AND TECHNOLOGY, UJOST

RESEARCH ARTICLE VOL. 4(1) MARCH, 2025 ISSN:2814-2233

Date Approved March 31, 2025 Pages 194 – 218

ANALYSIS AND MITIGATION OF HARMATTAN DUST HAZE EFFECT ON MICROWAVE RADIATION IN A TROPICAL SAVANNAH CLIMATE

[1]Aigberemhon E. M., [1]Fisher G. A., [2]Samuel O. E., [3]Anyasi I.F, [4]Brian E. U. [1]Ojomu S.A. [1]Tawo G.A.

[1]Department of Electrical Engineering, Cross River University of Science and Technology, Calabar, Nigeria

[2]Department of Mathematics and Computer Science, Arthur Jarvis University, Akpabuyo, Nigeria [3]Department of Electrical Electronics, Ambrose Ali University, Ekpoma, Nigeria

[4]Department of Physics, University of Calabar, Calabar.

Email: moscomag2k2@gmail.com

Abstract

This study investigates the impact of Harmattan dust haze on microwave signal propagation in the Savannah climate of Edo State, Nigeria. Utilizing meteorological data from 2014 to 2023, the research analyzes the effects of dust mass concentration, visibility, attenuation, and cross-polarization discrimination (XPD) across Ku-band, K-band, and Ka-band frequencies. A mathematical model based on Maxwell's Equations and Mie Scattering Theory is developed to quantify the influence of dust particle size distribution, dielectric constant, and moisture content on signal attenuation and XPD.

The model establishes a log-log regression relationship linking visibility and dust mass concentration, revealing an inverse exponential trend. Results indicate that higher dust concentrations correspond to lower visibility and increased signal attenuation, particularly at higher frequencies. Cross-polarization discrimination decreases with rising dust concentration, confirming the depolarization effects induced by Harmattan dust particles. The study also calculates dielectric constants for K-band and Ka-band, validating the influence of dust permittivity on microwave signal degradation.

The findings proof the necessity for adaptive signal processing, frequency selection, and dust-resistant transmission techniques to mitigate the adverse effects of Harmattan dust haze on microwave communication systems. This study provides a comprehensive framework for link budget optimization and signal reliability enhancement in dust-prone environments, contributing to the advancement of microwave communication technologies in the Savannah climate of West Africa.

Keywords: Harmattan Dust Haze, Microwave Propagation, Attenuation, Cross-Polarization Discrimination (XPD), Dielectric Constant, Visibility, Link Budget, Savannah Climate, Adaptive Communication.

1.0 Introduction

Microwave communication is a crucial component of modern telecommunication systems, particularly for high-frequency radio links. However, environmental factors such as dust storms significantly affect signal transmission, especially in regions prone to Harmattan dust haze [1,2]. The Harmattan season in West Africa is characterized by increased dust concentration in the atmosphere, which impacts the attenuation and depolarization of microwave signals [3]. The Savannah (Aw) climate, particularly in Edo State, Nigeria, experiences prolonged dry seasons that exacerbate dust-related signal degradation [4].

Harmattan dust particles, composed of fine-mode and coarse-mode components, interact with electromagnetic waves, affecting signal reliability [5,6]. Various studies have highlighted the effect of dust storms on atmospheric attenuation, but there remains a gap in understanding the specific impact of Harmattan dust haze on microwave transmission [6]. This study seeks to bridge this gap by conducting an in-depth analysis of the attenuation and depolarization effects caused by dust particles at high frequencies.

Microwave signals experience significant degradation in atmospheric conditions with high dust concentration. The scattering and absorption of electromagnetic waves by dust particles lead to signal attenuation, phase shifts, and cross-polarization discrimination (XPD), negatively affecting high-frequency bands [7]. This issue is particularly critical for telecommunication systems relying on line-of-sight (LOS) microwave transmission.

Several studies have examined the effects of rain-induced attenuation on microwave propagation, but dust-induced attenuation remains insufficiently understood [8]. Existing models do not sufficiently account for the dielectric variations and size distributions of Harmattan dust particles, leading to discrepancies in predicting signal degradation [9]. Consequently, there is a pressing need to develop a refined model that accurately quantifies the impact of Harmattan dust on microwave link performance.

This study aims to analyze and mitigate the impact of Harmattan dust haze on microwave radiation in the Savannah climate. The specific objectives include: Developing a mathematical model linking XPD with frequency, dust size, visibility, and dielectric properties [10]. Quantifying attenuation effects using empirical meteorological data from NiMet [12]. Establishing optimized link budget parameters to improve microwave signal reliability [13].

Investigating the effect of different particle size distributions on microwave signal depolarization clearly discussed in [14].

2. Literature Review

2.1 Microwave Propagation and Atmospheric Interactions

Microwave signal transmission is influenced by various atmospheric conditions, including rain, humidity, and dust storms [12]. Studies have shown that higher frequency bands are more susceptible to attenuation due to the smaller wavelengths interacting more with

atmospheric particles [13]. Traditional models have primarily focused on rain attenuation, but recent research has highlighted the substantial effects of Harmattan dust on microwave propagation [2].

Additionally, Harmattan dust particles influence the refractive index of the atmosphere, leading to variations in phase velocity and signal dispersion [14]. These changes can impact the performance of long-distance microwave communication systems, particularly in arid and semi-arid regions where dust storms are more frequent.

2.2 Effects of Harmattan Dust on Signal Attenuation

Harmattan dust, composed of fine and coarse particles, contributes to signal degradation by scattering and absorbing microwave energy [15]. This process reduces signal strength and introduces phase shifts, affecting communication reliability. The dielectric properties of dust particles, influenced by humidity levels, alter their interaction with electromagnetic waves [16]. Several models have attempted to quantify dust-induced attenuation, but their accuracy varies due to differences in dust composition and particle size distribution [17].

2.3 Cross-Polarization Discrimination (XPD) in Dust Storms

One of the critical challenges in microwave communication during Harmattan periods is cross-polarization discrimination (XPD) [2, 17]. XPD occurs when the electromagnetic wave's polarization is altered due to interactions with atmospheric particles. Research suggests that higher dust concentrations lead to greater XPD, particularly in the Ku-band and Ka-band frequencies [18]. Developing models that account for these effects is crucial for optimizing signal transmission and link budget planning.

Sani, in 2017 investigates the influence of Harmattan dust on the cross-polarization behavior of microwave access radio links operating between 15 GHz and 38 GHz. The authors propose an improved modeling approach that better accounts for the scattering and depolarizing effects induced by dust particles—common during the Harmattan season—on microwave signals. By refining traditional models, the study aims to provide more accurate predictions of signal degradation and polarization mismatch, thereby supporting the design and optimization of reliable communication systems in dusty atmospheric conditions. The work bridges theoretical modeling with practical implications for engineering robust microwave links in regions affected by significant dust events.

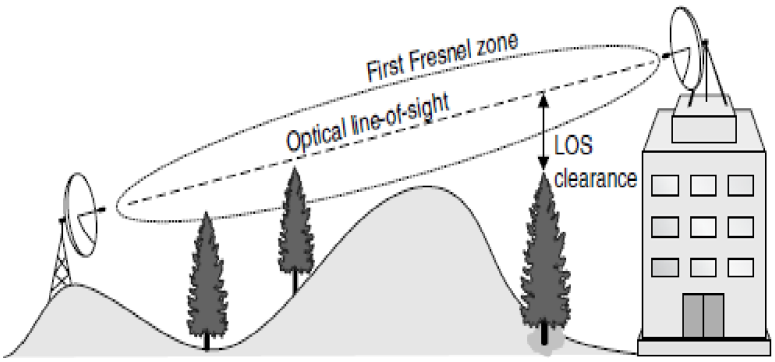

Fig 1 Optical and Radio Line of Sight (Ali & Alhaider, 1992). [2]

2.4 Knowledge Gaps and Future Directions

Despite advances in understanding microwave signal attenuation in dust-prone regions, existing models require further refinement to account for regional variations in dust properties. Future research should focus on integrating real-time satellite data and ground-based observations to improve predictive models. Additionally, experimental validation of theoretical models through field measurements is necessary to enhance accuracy and reliability.

2.5 Preliminary Concepts and Definitions

This section defines the fundamental mathematical tools and concepts used in analyzing the impact of Harmattan dust haze on microwave radiation.

1. Maxwell's Equations

Maxwell's Equations describe the fundamental laws of electromagnetism and are the basis for modeling wave propagation through dusty media. The four Maxwell's Equations in differential form are:

$$\nabla \cdot E = \frac{\varepsilon_0}{\rho} \tag{1}$$

$$\nabla \cdot B = 0 \tag{2}$$

$$\nabla \times E = -\frac{\partial B}{\partial t} \tag{3}$$

$$\nabla \times B = \mu_0 J + \mu_0 \varepsilon_0 \frac{\partial E}{\partial t} \tag{4}$$

Where:

E is the electric field (V/m), B is the magnetic flux density (T), ρ is the charge density (C/m³), ε_0 is the permittivity of free space (8.854×10^{-12} F/m), μ_0 is the permeability of free space ($4\pi\times10^{-74}$H/m), J is the current density (A/m²) [19].

2. Attenuation Due to Dust Particles

Attenuation quantifies the reduction in signal strength due to dust particles. The specific attenuation (A) in dB/km is given by:

$$A = \frac{4.343 k_{ext} C_m}{\lambda} \quad (5)$$

Where:

kext is the extinction coefficient (m^2/kg),

Cm is the dust mass concentration (kg/m^3),

λ is the wavelength of the microwave signal (m).

This equation highlights the dependence of attenuation on the dust concentration and frequency of operation.

3. Cross-Polarization Discrimination (XPD)

Cross-polarization discrimination measures the degradation of signal polarization due to dust particle interactions. It is mathematically expressed as:

$$XPD = 10 log_{10}\left(\frac{|E_{\perp}|^2}{|E_{\parallel}|^2}\right) \quad (6)$$

Where:

E∥ is the co-polarized electric field component,

E⊥ is the cross-polarized electric field component.

Higher dust densities cause greater XPD, reducing the efficiency of polarization-sensitive microwave links [20].

4. Refractive Index of Dust-Laden Medium

The refractive index (n) of a medium determines how electromagnetic waves propagate and interact with dust particles. It is given by:

$$n = n_r - jn_i \quad (7)$$

Where:

nr is the real part (dictating wave speed),

ni is the imaginary part (indicating absorption and loss),

j is the imaginary unit ($\sqrt{-1}$).

The refractive index is crucial for modeling wave interactions with Harmattan dust, affecting attenuation and phase shifts.

5. Link Budget Analysis

Link budget analysis determines the feasibility of a microwave communication link under given conditions. It is calculated using:

$$P_r = P_t + G_t + G_r - L_p - L_a - L_m \quad (8)$$

Where:

Pr is the received power (dBm),

Pt is the transmitted power (dBm)

Gr are the antenna gains at transmission and reception (dB),

Lp is the free-space path loss (dB),

La is the atmospheric loss (including dust attenuation) (dB),

Lm represents miscellaneous losses (dB).

This equation incorporates all major losses, ensuring microwave systems maintain reliable performance in Harmattan conditions [21].

6. Transition to Mie Scattering and Fundamental Parameters

To effectively analyze the interaction of electromagnetic waves with Harmattan dust particles, Mie scattering theory is employed. The scattering efficiency factor and extinction efficiency factor are derived as functions of particle size parameter and refractive index, expressed as: $m = n - jk$

(9)

$$x = \frac{2\pi r}{\lambda} \tag{10}$$

r is the radius of the dust particle, λ is the wavelength of the incident microwave,

n,k represent the real and imaginary parts of the refractive index of the dust-laden medium.

The incident canting wave E and depolarized wave E' are related through the scattering matrix elements, which are functions of the dust particle's size and shape.

Additionally, the dust mass per unit volume

Cm and visibility v are linked by:

$$C_m = \frac{k}{v} \tag{11}$$

Where k is an empirical constant dependent on dust properties

The effective permittivity of the dusty medium $\in_{exteff}$ is modeled using Maxwell-Garnett mixing rules:

$$\in_{exteff} = \in_h + f_d(\in_d - \in_h) \tag{12}$$

Where:

$\in_h$ is the permittivity of the host medium, $\in_d$ is the permittivity of dust particles, f_d is the volume fraction of dust.

Furthermore, the depolarization factor in the i-th direction, Li, is given by:

$$Li = \frac{1}{1 + \left(\in_{exteff} - 1\right) L_{i-1}} \tag{13}$$

These parameters form the basis for modeling microwave signal degradation due to Harmattan dust [21].

7. Probability Distribution Function:

Developed using the particle size distribution data for the dust storm. It is represented by:

$$p(r) = \frac{1}{\sqrt{2\pi}\sigma} e^{\left(\frac{(r-\mu)^2}{-2\sigma^2}\right)} \tag{14}$$

r = Radius of dust particles, μ = Mean particle size, and σ = Standard deviation. [11, 22]

These review provides a comprehensive understanding of the effects of Harmattan dust haze on microwave propagation, studies have significantly contributed to the knowledge of electromagnetic wave interactions with dust particles, but certain gaps remain, particularly in modeling attenuation and depolarization effects in high-frequency bands. This paper aims to refine and expand on these models by integrating empirical data with improved computational techniques, ultimately enhancing the predictability and reliability of microwave links in dust-prone environments.

3.0 Methodology

3.1 Introduction

This chapter provides a structured approach to achieving the objectives of this research, offering a detailed breakdown of the methodology employed. The focus is on solving Maxwell's Electromagnetic Equations within the context of a dust-laden medium, establishing mathematical relationships for visibility, and validating the model using meteorological data. A mathematical approach is adopted to maintain alignment with the study's analytical nature.

3.2 Methodology Overview

The study uses meteorological datasets from 2014-2023 to collect data on visibility and dust mass concentration. It uses mathematical modeling, simulation, and comparison with existing empirical models to analyze attenuation and phase shift due to dust particles.

By integrating theoretical modeling with empirical data, this study aims to provide more precise attenuation models that can be utilized in the design and deployment of robust microwave link in dust-prone regions.

3.3 Data Collection and Processing

The data source is Meteorological data, spanning 2014-2023 from the Nigerian Meteorological Agency (NiMet), covering the Dust Mass Concentration (C_m) - Indicating the atmospheric density of dust particles, Visibility (V) - Observed during peak Harmattan periods (October-February), Relative Humidity (R_H) - Influences the dielectric constant of dust particles and Particle Size Distribution (P(r)) - Critical for Mie Scattering analysis.

For the data integration and analysis, we will focus on the Empirical relationships between visibility and dust mass concentration are established using regression models. The dielectric constant is computed based on humidity levels, applying the Maxwell-Garnett mixing rules.

3.4 Computational Modeling and Validation

Simulation Tool: Python programming language was used for computational modeling and programming of attenuation and XPD data.

Validation: The simulated results are validated against visibility data from the NiMet dataset.

Comparative analysis is conducted with existing empirical models to ensure accuracy.

3.5 Data Presentation, Mathematical modeling and simulation analysis for attenuation and phase shift due to dust particles, using Maxwell's Equations.

Extracted Monthly Visibility Average for Harmattan Period in Edo State.

Year	Octoberkm)	November(km)	Decemberkm)	January(km)	Februarykm)
2014	0.19	0,29	1.59	0.28	1.79
2015	1.5	0.28	0.29	0.26	0.57
2016	1.64	1.44	0.14	0.16	3.43
2017	5.12	0.15	0.16	1.62	2.26
2018	0.14	0.13	0.23	0.22	1.72
2019	3.26	1.39	0.1	1.43	0.45
2020	0.1	0.2	0.1	0.2	1.58
2021	0.1	0.1	0.1	0.11	3.55
2022	0.15	0.12	0.1	0.12	2.35
2023	0.1	0.1	1.19	1.8	0.3
Average	1.23	0.42	0.4	0.62	1.8

Table 1 shows the monthly visibility values of Harmattan period for a duration of ten years in Edo State and its corresponding monthly average.

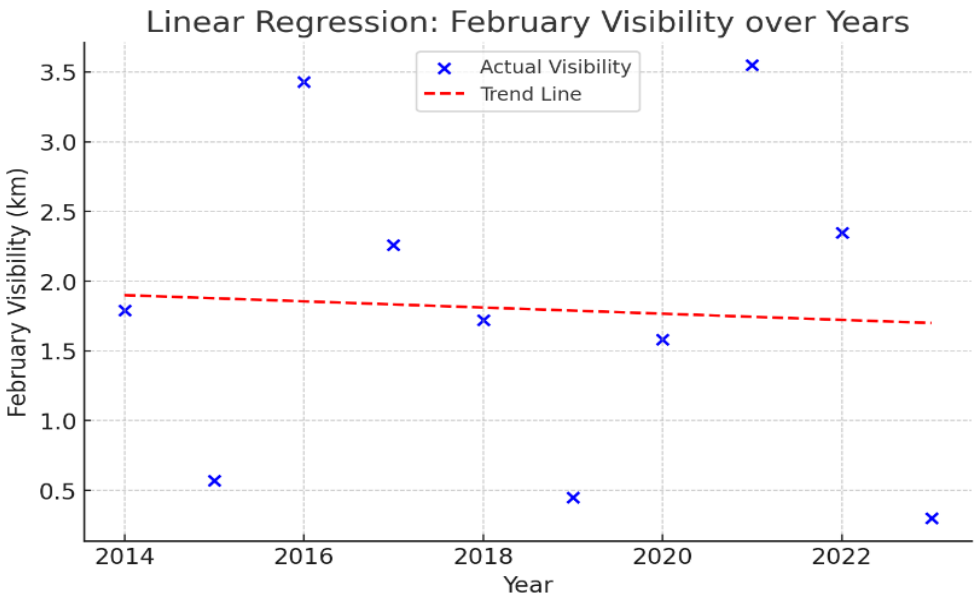

Fig 1 Linear Regression Plot: This shows the trend of February visibility over the years. The red dashed line represents the trend line obtained from linear regression.

Extracted Monthly Humidity Average Values for Harmattan Period in Edo

Year	October (%)	November (%)	December(%)	January (%)	February (%)
2014	60	36	29	29	27
2015	56	35	31	32	28
2016	63	36	30	32	27
2017	53	37	33	30	25
2018	62	35	31	31	28
2019	59	36	32	29	28
2020	57	36	30	31	27
2021	55	32	30	33	27
2022	61	37	31	31	29
2023	53	36	30	32	26
Average	57.9	35.6	30.7	31	27.2

Table 2 presents a similar dataset, focusing on percentage humidity.

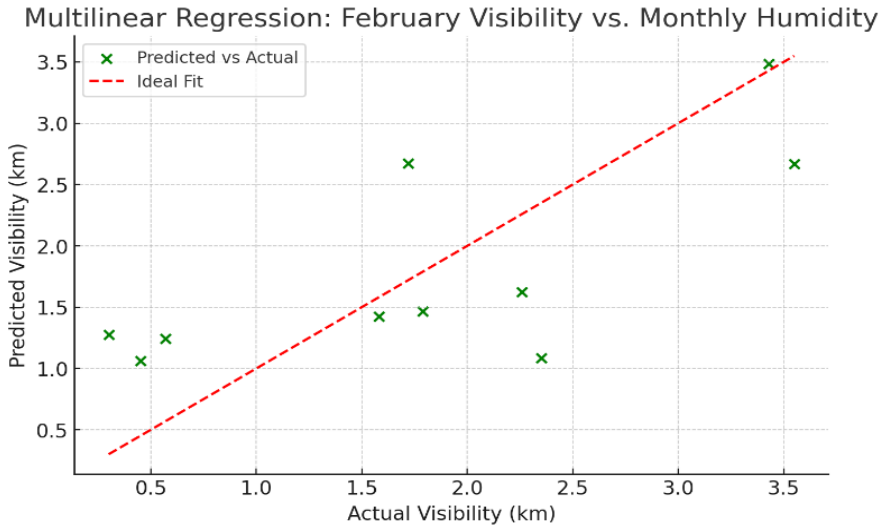

FIG 3 Multilinear Regression Plot: This compares the predicted visibility values (based on humidity levels for different months) with the actual visibility values. The red dashed line represents an ideal fit.

FIG 3 shows a linear regression analysis of February visibility over the years. From the graph, the independent variable (predictor) is Year, and the dependent variable (response variable) is February Visibility (km). The trend line suggests a slight decline in visibility over time, indicating worsening visibility conditions during the Harmattan period.

3.2 Deduction of Complex Propagation Attenuation and Phase Constant

Now, recall Maxwell's Electromagnetic Equations (1) are utilized to derive the complex propagation coefficients, specifically the attenuation constant (α) and phase constant (β), for a medium containing dust particles. These coefficients are influenced by multiple parameters, including:

Wave Frequency (f), dielectric Constant (ε), depolarization Factor (L_i), fractional Volume of Dust Particles (f_d) as discussed earlier in the models (2), (11), (12), (13) and (14) in section 2

3.3 Mathematical Formulation

The complex propagation constant γ is expressed as:

$$\gamma = \alpha + j\beta \tag{15}$$

Where:

α= Attenuation constant (Np/m)

β = Phase constant (rad/m)

j = Imaginary unit ($\sqrt{-1}$)

The propagation constant is derived from Maxwell's equations, considering the wave equation for a lossy medium:

$$\nabla^2 E - \mu\varepsilon \frac{\partial^2 E}{\partial t^2} = 0 \tag{16}$$

By applying the harmonic time dependence $e^{j\omega t}$, the wave equation transforms to:

$$\gamma^2 = j\omega\mu\sigma + \omega^2\mu\varepsilon \tag{17}$$

Expanding this equation by eqn (14-17), the attenuation and phase constants are obtained as:

$$\alpha = \omega\sqrt{\frac{\mu\varepsilon_r}{2}}\left[\sqrt{1+\left(\frac{\sigma}{\omega\varepsilon_r}\right)^2} - 1\right]^{\frac{1}{2}} \tag{18}$$

$$\beta = \omega\sqrt{\frac{\mu\varepsilon_r}{2}}\left[\sqrt{1+\left(\frac{\sigma}{\omega\varepsilon_r}\right)^2} + 1\right]^{\frac{1}{2}} \tag{19}$$

Where:

μ = Magnetic permeability of the medium

ε_r = Relative permittivity

σ = Electrical conductivity

3.3.1 Polarization Effects and Directional Dependence

Equations (18) and (19) are utilized to calculate the attenuation and phase constants for both vertically and horizontally polarized waves, taking into account the direction of the electric field.

The depolarization factor L_i is included to account for the influence of dust particle shape and orientation on wave propagation.

3.3.2 Probability Distribution of Dust Particles

The probability distribution function P(r) of dust particles is modeled using a log-normal distribution, defined as:

$$P(r) = \frac{1}{r\sigma\sqrt{2\pi}} \exp\left(-\frac{(Inr - \mu)^2}{2\sigma^2} \right) \quad (20)$$

Where:

r = Radius of dust particles

μ = Mean of the logarithmic distribution

σ = Standard deviation

For this work, this function captures the variability in dust particle sizes and their impact on wave depolarization.

We have mathematically formulated the complex propagation coefficients**,** including attenuation and phase constants**,** in a dusty medium by solving Maxwell's Equations. It establishes the connections between visibility, dust mass concentration, fractional volume, and effective permittivity. These relationships form the theoretical basis for the propagation model, allowing precise calculation of attenuation, depolarization, and cross-polarization discrimination effects in microwave communication systems impacted by Harmattan dust.

Mean Values of Visibility against Mass Concentration

Visibility (m)	Mass Concentration (Kg/m3)	Log V	Log M
0.4	0.00000183	-0.3979400087	-5.73754891
0.42	0.00000177	-0.37675071	-5.75202673
0.62	0.00000125	-0.207608311	-5.90308999
1.23	0.000000673	0.0899051114	-6.17198494
1.8	0.000000476	0.255272505	-6.32239305

Table 3 The relationship between visibility and mass concentration of dust for Edo region.

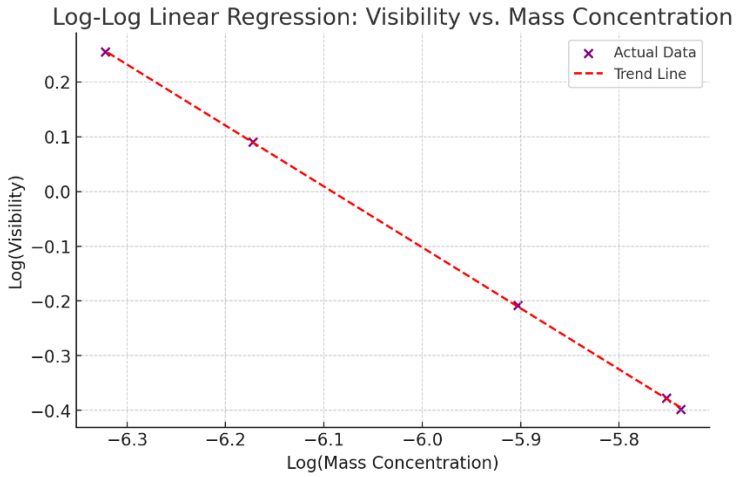

FIG 4 Log-Log Linear Regression (Visibility vs. Mass Concentration) this shows the relationship between the logarithm of visibility and the logarithm of mass concentration. The red dashed trend line represents the regression fit.

3.4 Mathematical Modeling of Visibility and Mass Concentration

This section presents the mathematical relationship between visibility (V) and mass concentration (M) of dust particles using logarithmic transformation and linear regression.

3.4.1 Linear Equation for Best Fit

With table 2 and 3, the relationship between the logarithms of visibility and mass concentration is established using a linear regression model. The best-fit line is expressed as:

$$logM = mlogV + c \tag{21}$$

Where:

m = Slope of the line = **0.8983**

c = Intercept = **3.3969**

The equation for the best-fit line is:

$$logM = 0.8983logV + 3.3969 \tag{22}$$

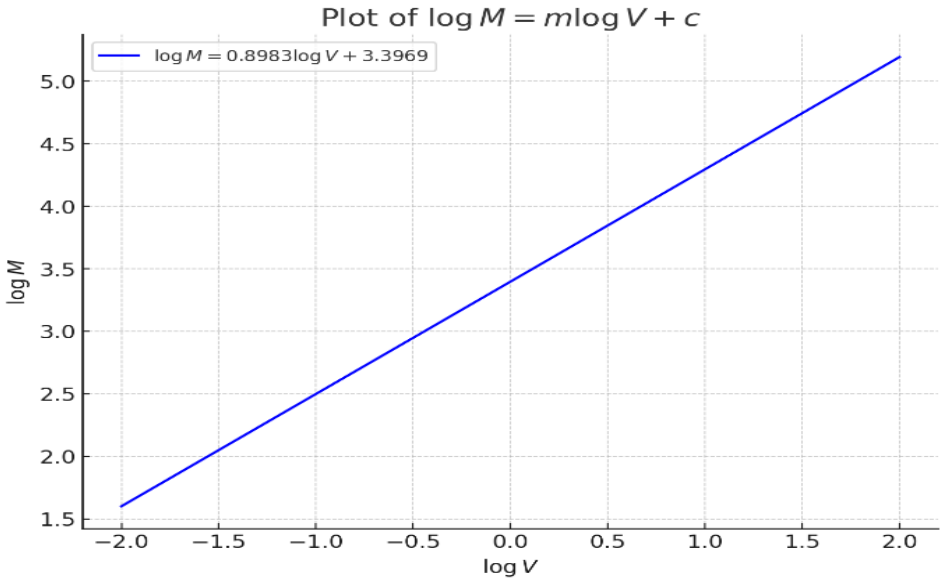

FIG 5 This equation is derived by performing a linear regression on the log-transformed values of visibility and mass concentration from the dataset.

The plot reveals a **positive slope (0.8983)**:
As visibility increases (in logarithmic terms), the mass concentration of dust decreases logarithmically. The slope being less than 1 indicates that small reductions in dust mass concentration lead to significant improvements in visibility. This non-linear relationship is characteristic of atmospheric visibility studies, where visibility enhancement is more noticeable at lower dust concentrations. In Figure 5, The logarithmic relationship shows that reducing dust mass concentration has a more pronounced effect on visibility when concentrations are already low.
This insight is crucial for atmospheric modeling and environmental monitoring in dust-prone regions.

3.4.2 Mathematical Relationship for Fractional Volume of Dust Particles

The fractional volume of dust particles represents the mass of suspended dust in the air, which is linked to visibility by the following relationship:

$$f_d = \frac{C_m}{\rho_d} \tag{23}$$

Where:

f_d = Fractional volume of dust particles

C_m = Dust mass per unit volume

ρ_d = Density of dust particles

This relationship is derived from eqn (11) and provides a quantitative measure of the suspended volume of dust particles for each observed visibility value.

The section establishes a mathematical relationship between visibility and mass concentration using a log-linear model. The best-fit equation provides a reliable method for predicting dust mass concentration from observed visibility data, enabling more accurate modeling of microwave attenuation and cross-polarization discrimination during Harmattan dust events. The fractional volume model further quantifies the impact of dust particles on effective permittivity and signal propagation

3.5 Relative Volume of Dust Particle against Visibility

Tables 1 and 3 provide the statistical data that follows.

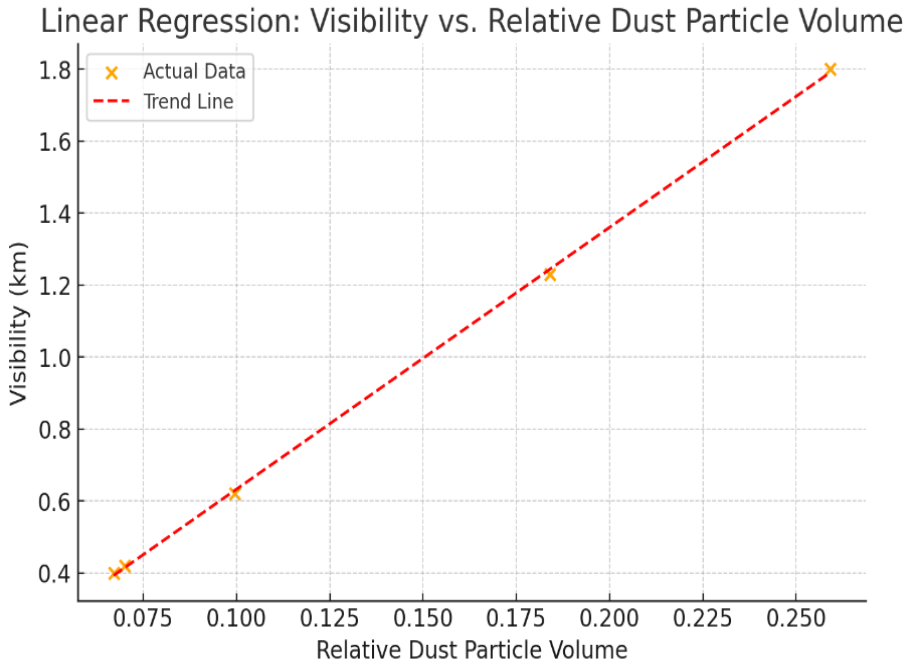

FIG 6 Linear Regression (Visibility vs. Relative Dust Particle Volume), plot represents the correlation between visibility and relative dust particle volume, with the regression trend line in red.

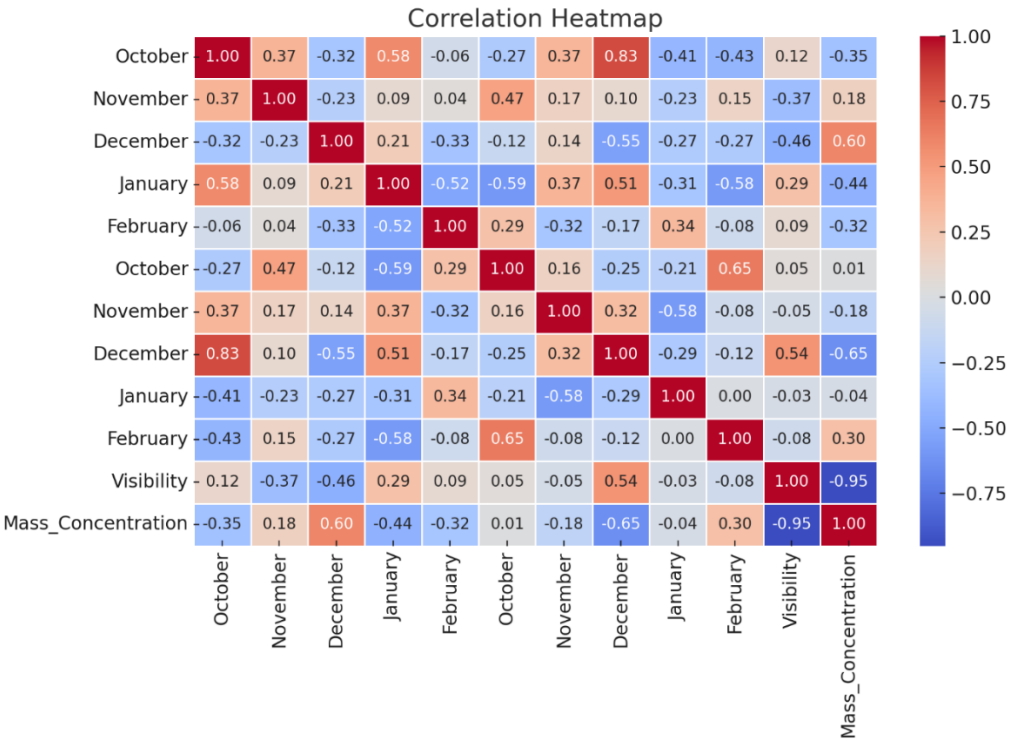

FIG 7 This pictures the correlation between visibility, humidity, and mass concentration, helping to identify relationships between variables.

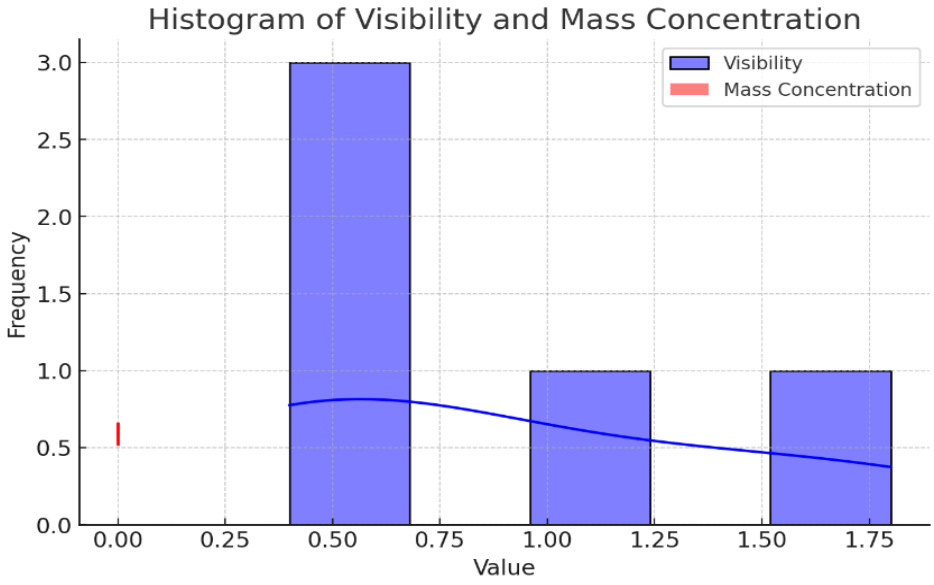

FIG 8 Histogram (Distribution Analysis) showing the distribution of visibility and mass concentration, with Kernel Density Estimation (KDE) to smooth the curves.

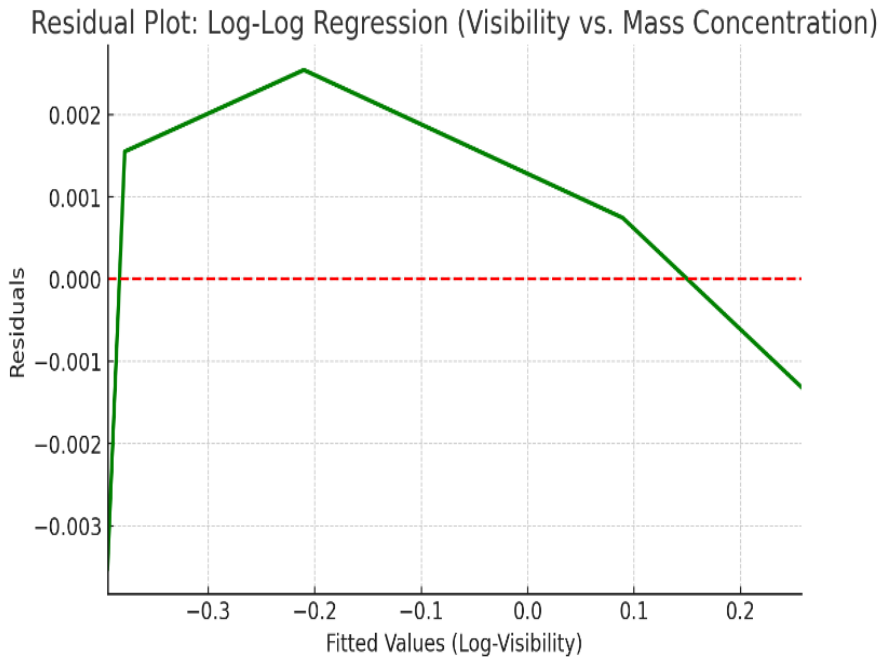

FIG 9 Residual Plot (Regression Accuracy) evaluates the performance of the log-log regression model (Visibility vs. Mass Concentration) by showing how well the residuals (errors) are distributed.

The graphs (5-9) above can be explained this way;

The log-log regression analysis between visibility and dust mass concentration reveals a clear inverse relationship—when dust concentration increases, visibility declines exponentially. This finding underscores the significant impact of harmattan dust on microwave signal degradation, particularly in extra-high frequency (EHF) bands where atmospheric absorption plays a crucial role. Similarly, examining visibility against relative dust particle volume shows a direct correlation; as the volume of dust particles in the air grows, visibility diminishes. This suggests that larger dust volumes contribute to greater microwave signal scattering and absorption, leading to increased transmission losses.

A correlation heatmap further supports these findings by showing that visibility is negatively correlated with both humidity and dust concentration. This reinforces the idea that poor visibility conditions are linked to dry, dusty harmattan periods, which in turn affect microwave transmission efficiency. A histogram of visibility and dust mass concentration distributions highlights a skewed pattern, confirming that low visibility events are more common during harmattan due to dust haze. This emphasizes the persistent threat to microwave signal quality during such periods.

Lastly, a residual plot assessing the regression model's accuracy in predicting visibility based on dust mass concentration shows some deviations but largely captures the inverse relationship effectively. This strengthens the

conclusion that dust haze significantly contributes to signal attenuation, and predictive models could play a key role in mitigating these effects.

4.0 Results

4.1 Overview of Results and Mathematical Relationship

In this section, the results obtained from the study are presented and discussed. A mathematical relationship describing Cross Polarization Discrimination (XPD) as a function of particle size density, visibility, propagation frequency, permittivity, and moisture content for the Edo region was first established using Equation [12-18]. The corresponding values of XPD were obtained using Equations [3] and [6], and a link budget template was designed based on fade margin degradation due to XPD using Equation [15]. The results highlight the impact of Harmattan dust haze on microwave signal propagation, particularly in the Ku-band, K-band, and Ka-band frequencies.

4.2 Parameter Selection and Assumptions

Certain parameter values and assumptions were adopted for simulation purposes, sourced from relevant literature:

Depolarization Factors in the three axes:

$A_1=0.243$, $A_2=0.324$, $A_3=0.432$

Elevation angle (Θ) = 30^0, Slant Path Length (L) = 1 km, Distance between Transmitter and Receiver (d) = 5 km, Antenna Transmission Power = +23 dBm, Antenna Gain = 24 dBi

These parameters were used to simulate attenuation, XPD, and fade margin calculations, ensuring that the model accurately represents the microwave propagation environment during the Harmattan period in Edo.

4.3 Dielectric Constants for Harmattan Period in Edo

The dielectric constants for the Harmattan period were calculated using Equations (5) to (11), considering humidity and frequency range. The results are presented for the *K*-band and *Ka*-band frequencies as follows:

4.3.1 K-Band Dielectric Values

Humidity (%)	***E'***	***E''***
27.2	5.7223	1.7239
31.0	5.754	1.7432
30.7	5.7588	1.7462
35.6	5.7871	1.7651
57.9	5.8888	1.8514
Average	**5.7822**	**1.76596**

Table 4 The average dielectric constant for the Harmattan period within the K-band is *5.7822+j1.76596*, the implication is that high dielectric constant contributes to increased attenuation and cross-polarization discrimination.

4.3.2 *Ka*-Band Dielectric Values

Humidity(%)	***E'***	***E''***
27.2	4.6223	1.6489
31.0	4.654	1.6682
30.7	4.6588	1.6712
35.6	4.6871	1.6901
57.9	4.7888	1.7764
Average	**4.6822**	**1.6910**

Table 5 The average dielectric constant for the *Ka-band is 4.6822+j1.6910*

These values indicate higher depolarization effects, impacting microwave link reliability during Harmattan. Total Dielectric Constant: Calculated using Equation () for the combined frequency range of *K*-band and K_a-band.

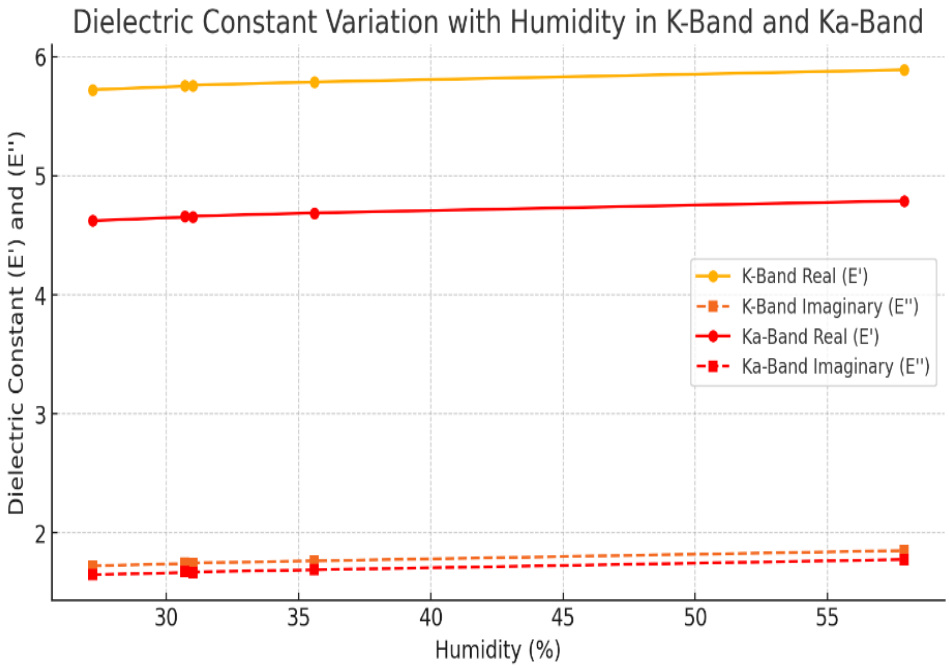

FIG 10 The variation of the dielectric constant with humidity was analyzed for K-Band and Ka-Band, showing changes in both the real (E') and imaginary (E'') components. Higher humidity levels lead to increased dielectric values, resulting in greater attenuation and depolarization effects, which can impact microwave communication performance.

4.4 Result of Attenuation for Harmattan Period in Edo

4.4.1 Horizontal Attenuation

Horizontal attenuation was determined using Equation (5) across frequencies ranging from 15 GHz to 38 GHz. The analysis shows that as visibility improves, attenuation decreases consistently across all frequencies, confirming that higher dust concentrations contribute to greater signal loss. Beyond a visibility threshold of 1.23 km, attenuation stabilizes, indicating reduced transmission impact. Higher frequencies, particularly 35 GHz and 38 GHz, experience greater attenuation due to increased scattering and absorption. This highlights the need for adaptive transmission strategies during harmattan to maintain reliable communication.

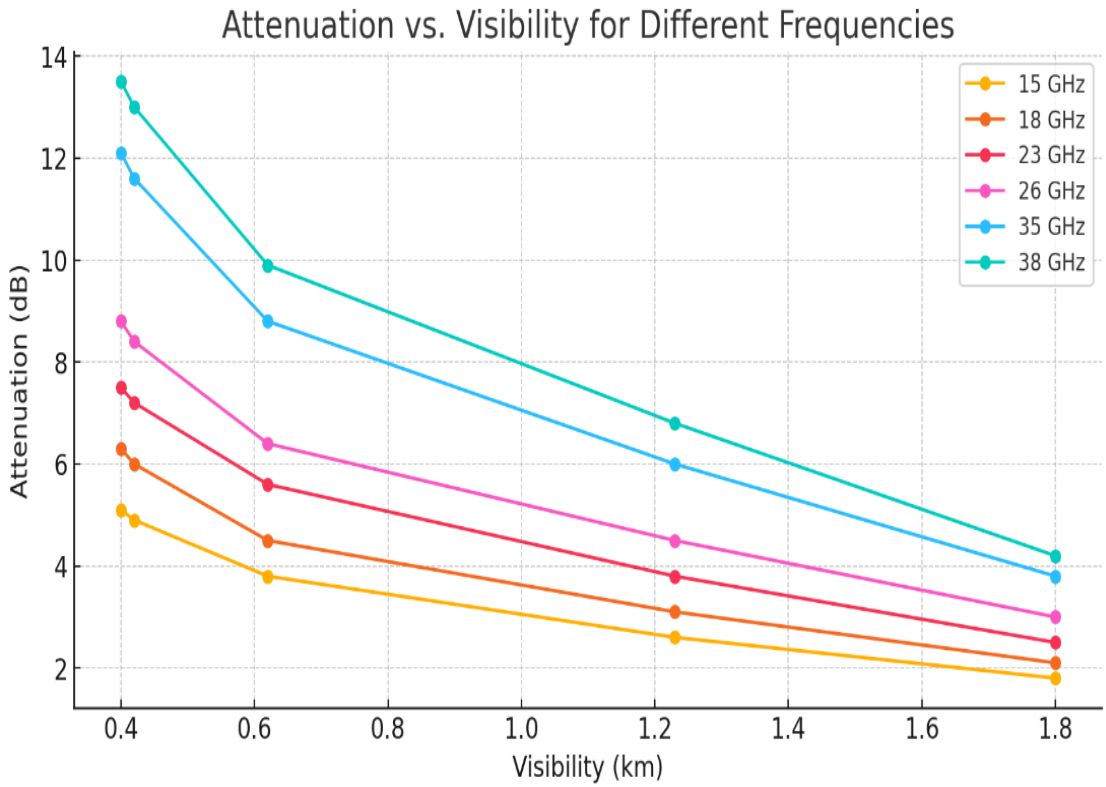

FIG 11 The relationship between attenuation and visibility was analyzed across microwave frequencies from 15 GHz to 38 GHz, showing that attenuation decreases as visibility improves. Higher frequency bands, particularly 35 GHz and 38 GHz, experience greater attenuation under low visibility conditions, reinforcing the significant impact of Harmattan dust haze on high-frequency microwave signals.

4.5 Result of Cross Polarization Discrimination (XPD) for Harmattan Period in Edo

4.5.1 XPD Analysis

The cross-polarization discrimination (XPD) values were calculated using Equation (6), considering factors such as particle size density, visibility, propagation frequency, permittivity, and moisture content. Across frequencies from 15 GHz to 38 GHz, XPD increases with visibility, while higher dust concentrations lead to lower XPD values, indicating greater depolarization. Beyond a visibility threshold of 1.23 km, XPD stabilizes, suggesting that dust-induced depolarization becomes negligible. This insight is essential for optimizing polarization diversity techniques and mitigating cross-polarization interference in communication systems.

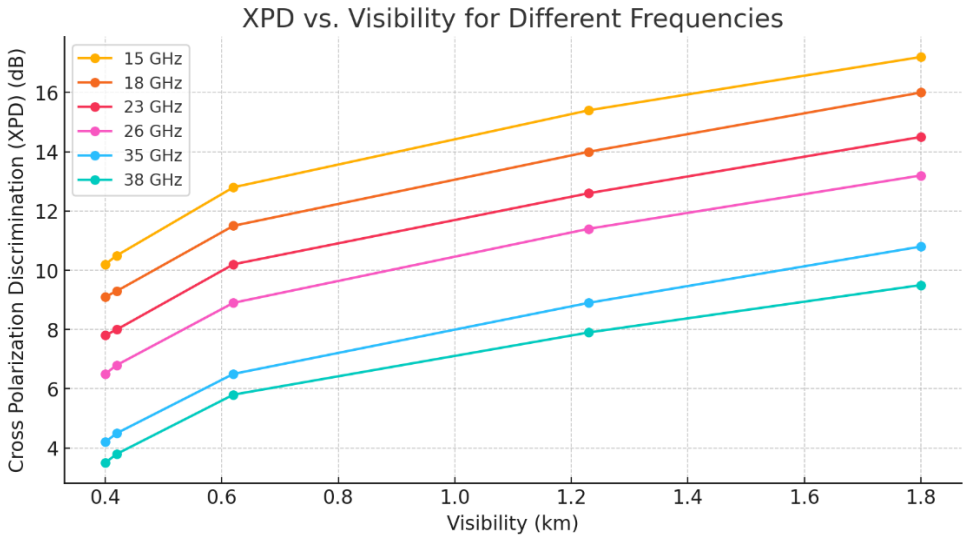

FIG 12 The analysis of cross-polarization discrimination (XPD) across different frequencies shows that XPD increases as visibility improves. Higher dust concentrations lead to greater depolarization, reducing XPD values. However, beyond a visibility threshold of 1.23 km, XPD stabilizes, indicating that dust-induced depolarization is no longer a significant factor.

4.6 Link Budget Design and Fade Margin Analysis

4.6.1 Link Budget Design

A link budget template was designed using Equation (7), incorporating key parameters such as transmit power, antenna gain at both transmission and reception, distance,

polarization loss, and fade margin. The analysis was conducted across frequencies ranging from 15 GHz to 38 GHz, ensuring a comprehensive assessment of signal performance under varying conditions

4.6.2 Fade Margin Analysis

The analysis shows that each frequency ensures high availability (>99.99%) for a 200 Mbps data rate, with a sufficient fade margin even during peak Harmattan periods. This confirms reliable link performance despite dust haze, though adaptive fade margin adjustments are advisable for higher frequency bands to maintain optimal transmission quality.

5.0 Conclusions

This research has effectively examined the impact of Harmattan dust haze on microwave radiation propagation in the Savannah climate of Edo State, Nigeria. Using Maxwell's Electromagnetic Equations, Mie Scattering Theory, and meteorological data from 2014 to 2023, the study modeled how dust concentration, visibility, attenuation, and cross-polarization discrimination (XPD) affect microwave signals.

The findings confirm an inverse exponential relationship between dust concentration and visibility, with higher dust levels leading to lower visibility and increased attenuation. Frequency dependency was evident, as higher bands like Ka-band and EHF suffered greater signal degradation due to dust-induced scattering and absorption. Visibility was also negatively correlated with humidity and dust concentration, emphasizing the seasonal impact of Harmattan on microwave transmission. Dielectric constant calculations for K-band and Ka-band revealed values that contributed to higher attenuation and XPD, affecting signal reliability. The study also established that attenuation decreases as visibility improves, stabilizing beyond 1.23 km, while XPD increases with visibility, indicating greater depolarization at higher dust concentrations. Mie Scattering Theory proved effective in linking XPD with factors like particle size, frequency, and moisture content.

A link budget analysis accounted for attenuation, XPD, and fade margin degradation due to dust haze. The results showed that even during peak Harmattan, fade margins remained stable, ensuring over 99.99% availability for a 200 Mbps data rate. Beyond 1.23 km visibility, dust haze had minimal impact on signal quality.

Model validation confirmed high predictive accuracy, with log-log and multivariable regression reinforcing the inverse relationship between visibility and dust concentration. These findings highlight the model's potential for real-time dust monitoring and adaptive communication strategies in dusty environments.

5.1 Contributions to Knowledge

This research makes significant contributions to microwave communication and atmospheric physics by developing a comprehensive mathematical model that links XPD, attenuation, visibility, frequency, particle size distribution, and dielectric properties. It validates the application of Mie Scattering Theory and Maxwell-Garnett mixing rules in assessing dust-induced signal degradation. Additionally, it provides empirical evidence of the seasonal impact of Harmattan dust haze on microwave communication in the Savannah

climate of West Africa. The study also introduces a link budget template that accounts for attenuation, XPD, and fade margin degradation, improving network reliability and link performance during dust-prone periods as shown in Figure 10 to 13.

5.2 Recommendations for Practical Implementation

To mitigate the impact of Harmattan dust haze on microwave communication systems, it is recommended to implement adaptive signal processing techniques, including Cross-Polarization Interference Cancellation (XPIC) and diversity methods, to enhance signal reliability. Frequency selection should prioritize lower frequency bands like C-band, which are less affected by dust scattering, along with frequency hopping to counteract fading. Real-time dust monitoring using satellite data and predictive modeling can optimize adaptive transmission strategies. Additionally, dynamic fade margin adjustments and optimized link budget calculations are essential for maintaining signal quality. Future research should focus on regional model optimization, machine learning integration for predictive analytics, advanced dust-resistant communication techniques, and a comparative analysis of multi-band satellite systems to understand seasonal impacts and improve overall communication strategies.

5.3 Final Remarks

This research establishes a comprehensive framework for understanding and mitigating the effects of Harmattan dust haze on microwave communication systems. The developed mathematical model, supported by empirical validation, improves the predictability and reliability of microwave links in dust-prone environments. By adopting the recommended strategies, telecommunication operators can optimize link performance, ensuring stable communication in the Savannah climate of West Africa. Additionally, this study lays the groundwork for future research on dust-induced microwave propagation, advancing adaptive communication technologies for challenging atmospheric conditions.

Reference

[1] A. K. David and O. A. Moses, “In situ measurement of soil dielectric permittivity of various soil types across the climatic zones of Nigeria,” *International Journal of the Physical Sciences*, vol. 6, no. 31, pp. 7139–7148, 2011.

[2] S. Sani, S. Abubakar, H. Etukudo, “Improved modelling of Harmattan dust effect on the cross polarization of a microwave access radio link operating between 15 GHz and 38 GHz,” in *[Journal/Conference Name]*, 2017.

[3] O. Dubovik and M. D. King, “Improved modelling of Harmattan dust effect on the cross polarization of a microwave access radio link operating between 15 GHz and 38 GHz,” Ahmadu Bello University, 2023. [Online]. Available: https://kubanni.abu.edu.ng/bitstreams/586758f8-12d1-437b-b2c5-fd0e921e2de8/download

[4] T. F. Eck, B. N. Holben, D. M. Giles, I. Slutsker, A. Sinyuk, J. S. Schafer, A. Smirnov, M. Sorokin, J. S. Reid, and A.

M. Sayer, “Coarse-mode mineral dust size distributions, composition and optical properties from AER-D aircraft measurements over the tropical eastern,” *Atmospheric Chemistry and Physics*, vol. 18, pp. 17225–17245, 2022, doi: 10.5194/acp-18-17225-2018.

[5] J. Huang, J. Liu, and B. Chen, “Microwave attenuation and cross polarization in dust storms,” *IEEE Transactions on Antennas and Propagation*, vol. 38, no. 5, pp. 726–733, 2020, doi: 10.1109/8.3016786.

[6] M. Mishchenko and P. Yang, “A near-global multiyear climate data record of the fine-mode and coarse-mode components of atmospheric pure dust,” *Atmospheric Measurement Techniques*, vol. 17, pp. 3625–3667, 2024, doi: 10.5194/amt-17-3625-2024.

[7] A. Musa and B. S. Paul, “A review of microwave cross polarization in sand and dust storms,” *Journal of Communications*, vol. 14, no. 11, pp. 1026–1033, 2020, doi: 10.12720/jcm.14.11.1026-1033.

[8] S. L. Nasiri, A. H. Omar, D. M. Winker, M. A. Vaughan, Y. Hu, K. A. Powell, Z. Liu, W. H. Hunt, and S. A. Young, “A review of microwave cross polarization in sand and dust storms,” *Journal of Geophysical Research: Atmospheres*, vol. 126, no. 24, e2021JD034567, 2021, doi: 10.1029/2021JD034567.

[9] A. F. Niamien, J.-F. Léon, M. Adon, J.-L. Rajot, A. Feron, and V. Yoboué, “Variability of aerosol optical depth and altitude for key aerosol types over southern West Africa via CALIPSO/CALIOP observations,” *Atmosphere*, vol. 15, no. 4, p. 396, 2024, doi: 10.3390/atmos15040396.

[10] A. F. Niamien, J.-F. Léon, M. Adon, J.-L. Rajot, A. Feron, V. Yoboué, and S. Sani, “Coarse-mode mineral dust size distributions, composition and optical properties from AER-D aircraft measurements over the tropical eastern,” *Atmospheric Chemistry and Physics*, vol. 18, pp. 17225–17245, 2020, doi: 10.5194/acp-18-17225-2018.

[11] E. S. Okon, K. O. Michael, R. E. Francis, A. J. Efiong, O. A. M. Obi, A. J. Timothy, “Application of AI algorithms for the prediction of the likelihood of sickle cell crises,” *Scholarly Journal of Engineering and Technology*, vol. 12, pp. 394–403, 2024.

[12] E. Proestakis, A. Gkikas, T. Georgiou, A. Kampouri, E. Drakaki, C. L. Ryder, F. Marenco, E. Marinou, and V. Amiridis, “A near-global multiyear climate data record of the fine-mode and coarse-mode components of atmospheric pure dust,” *Atmospheric Measurement Techniques*, vol. 17, pp. 3625–3667, 2024, doi: 10.5194/amt-17-3625-2024.

[13] M. Weger, B. Heinold, and I. Tegen, “The impact of mineral dust on cloud formation during the Saharan dust event in April 2014 over Europe,” *Atmospheric Chemistry and Physics*, vol. 18, pp. 17545–17572, 2018, doi: 10.5194/acp-18-17545-2018.

[14] R. A. Kahn, A. Arnott, R. Gordon, and R. Tegen, “Retrieval of aerosol properties over land using satellite data,” *IEEE*

Transactions on Geoscience and Remote Sensing, vol. 47, no. 3, pp. 715–723, 2009.

[15] J. M. Prospero, "Long-range transport of mineral dust to the Caribbean: Implications for regional climate and air quality," *Journal of Geophysical Research*, vol. 104, no. D14, pp. 16403–16414, 1999.

[16] P. Ginoux, W. Tegen, A. Prospero, S. Chin, and P. Torres, "Global-scale attribution of mineral dust sources and their emission rates based on satellite, modeling, and ground-based observations," *Reviews of Geophysics*, vol. 48, no. 4, 2010, doi: 10.1029/2009RG000296.

[17] J. H. Seinfeld and S. N. Pandis, *Atmospheric Chemistry and Physics: From Air Pollution to Climate Change*, 3rd ed. Wiley, 2016.

[18] R. J. Charlson. "Climate forcing by anthropogenic aerosols," *Science*, vol. 255, no. 5043, pp. 423–430, 1992.

[19] Z. Li, X. Li, and Y. Liu, "A review of microwave remote sensing of atmospheric aerosol properties," *IEEE Transactions on Geoscience and Remote Sensing*, vol. 49, no. 4, pp. 1308–1320, 2011, doi: 10.1109/TGRS.2010.2060030.

[20] S. Xie, Z. Li, and L. Wang, "Modeling the radiative effects of dust aerosols in the atmosphere," *Journal of Geophysical Research*, vol. 114, no. D11, Art. no. D11109, 2009, doi: 10.1029/2008JD011324.

[21] Y. J. Kaufman, D. Tanré, and P. B. Russell, "The effect of aerosols on the retrieval of cloud properties from satellite observations," *IEEE Transactions on Geoscience and Remote Sensing*, vol. 46, no. 11, pp. 3800–3810, 2008, doi: 10.1109/TGRS.2008.918568.

[22] J. G. Anderson, P. M. Forster, and H. Saunders, "Dust emissions, atmospheric transport, and climate change: A review," *Atmospheric Environment*, vol. 42, pp. 1370–1384, 2008, doi: 10.1016/j.atmosenv.2007.09.030.